AI-Driven CAD for Histological Analysis in Mountain Regions: Advancing Local Healthcare and Sustainable Development

Matteo Calabrese[1,*], Chiara B. Salvemini[1], Michela Assale[1], Stefano Sartor[1], Roberta Patetta[2], Laura Caramanico[2], Andrea Cavalli[3,4], Stefano Gustincich[5,6] and Jean Marc Christille[1]

[1]*Fondazione Clément Fillietroz ONLUS, Astronomical Observatory of the Autonomous Region of the Aosta Valley (OAVdA), Nus, Italy*

[2]*Azienda USL della Valle D'Aosta, U. Parini Hospital, Struttura Complessa di Anatomia Patologica, Aosta, Italy*

[3]*Computational and Chemical Biology, Italian Institute of Technology (IIT), CMP[3] VdA, Aosta, Italy*

[4]*CECAM-EPFL, 1015 Lausanne, Switzerland*

[5]*Non-coding RNA and RNA-based therapeutics, Italian Institute of Technology (IIT), CMP[3] VdA, Aosta, Italy*

[6]*Non-coding RNA and RNA-based therapeutics, Center for Human Technology, Italian Institute of Technology (IIT), Genova, Italy*

Abstract

Accurate quantification of the Ki-67 proliferation index is essential in cancer diagnostics, yet manual evaluation remains time-consuming and prone to inter-observer variability. This study presents a machine vision-based CAD tool designed to compute Ki-67 proliferation index from digitized histopathological images, aiding diagnostic workflows at the U. Parini hospital in Aosta. Developed through an interdisciplinary approach integrating artificial intelligence and computational pathology, the system was validated against expert annotations, demonstrating strong concordance and clinical reliability. Beyond its scientific contributions, this initiative fosters digital transformation in healthcare, improving diagnostic accessibility in mountainous regions while promoting local economic and technological development.

Keywords

AI, Machine Vision (MV), Computer-Aid-Diagnostic (CAD), scientific research, local healthcare system, economic and social development.

1. Introduction

Artificial intelligence (AI) is revolutionizing healthcare by enhancing diagnostic accuracy, personalizing treatments, and expanding access to medical services, particularly in logistically-complex regions. In rural and mountainous areas, such as Italy's Aosta Valley, healthcare delivery faces unique challenges, including geographical isolation and limited medical resources. Implementing AI-driven solutions in these regions can bridge healthcare disparities by providing advanced diagnostic tools and supporting clinical decision-making.

Accurate assessment of cellular proliferation is crucial in cancer diagnostics, with the Ki-67 protein serving as a key biomarker. Traditionally, pathologists manually evaluate Ki-67 expression in histopathological images, a process that is time-consuming and susceptible to inter-observer variability. Computer-aided diagnosis (CAD) systems utilizing machine vision (MV) techniques have emerged to automate this task, offering consistent and efficient analysis of Ki-67 proliferation index.

The integration of such technologies is particularly significant in remote and mountainous regions. By deploying AI-driven diagnostic tools locally, these areas can undergo digital transformation, enhancing healthcare delivery and fostering collaborations between research centers, hospitals, and medical professionals. This synergy not only improves diagnostic practices but also contributes to the overall quality of life in these communities.

2nd Workshop "New frontiers in Big Data and Artificial Intelligence" (BDAI 2025), May 29-30, 2025, Aosta, Italy

*Corresponding author.

calabrese@oavda.it (M. Calabrese)

0000-0002-2637-2422 (M. Calabrese)

This paper presents a machine vision tool developed within the *CMP3 - 5000 genomi@vda*[1] project, designed to analyse histopathological images of breast cancer and compute the relative Ki-67 proliferation index. This tool has been implemented and deployed at the local hospital U. Parini in Aosta, enabling clinicians to utilize it as a supportive CAD system for their diagnostic processes. The objectives of this paper are to describe the machine vision tool and the CAD infrastructure, and to contextualize their development within the local setting. We aim to demonstrate how initiatives that link local research centers with healthcare institutions can promote collaboration, drive scientific and technological research, and enhance diagnostic practices, thereby improving the quality of life in mountainous regions like the Aosta Valley.

The structure of this paper is as follows: Section 2 contextualizes the scientific and aspects, providing a literature review on Ki-67 assessment and the need for CAD systems; Section 3 describes the MV algorithms and the data utilized; Section 4 presents the results, validation, and implementation of the solution in clinical practice; Section 5 offers a discussion on the findings and their implications; and Section 6 concludes the paper, summarizing the contributions and future directions.

2. Background and motivation

2.1. Scientific rationale

Early detection of breast cancer is crucial for improving patient survival and quality of life [1]. As the most common malignancy among women worldwide - with millions of new cases annually - efficient diagnostic tools are essential for managing clinical workloads and ensuring timely, accurate diagnoses. Diagnostic approaches include self- and clinical examinations, as well as imaging modalities such as mammography, ultrasound, and magnetic resonance imaging (MRI) [2, 3]. Mammography is the primary screening tool, while ultrasound and MRI are particularly useful in cases of dense breast tissue and complex presentations. Nonetheless, biopsy remains the definitive method for confirming a diagnosis [4, 5, 6]. However, challenges such as dense tissue and the potential for false-positive or false-negative results persist [7]. Ongoing research into advanced diagnostic techniques and molecular biomarkers promises to further improve the diagnosis and treatment of breast cancer [8, 9]. In the clinical practice, following tissue extraction through biopsy or surgical resection, histopathological analysis is conducted. This process involves preparing tissue sections and staining them - typically with Hematoxylin and Eosin (H-E) [10] or alternative markers such as DAB and Ki-67 [11] - to enhance cellular details before digitizing the slides into high-resolution images that play a vital role in clinical assessment [12].

Artificial intelligence (AI) applications in medical imaging have significantly advanced histopathology through Machine Vision (MV), enabling automated detection and quantification of biomarkers [13, 14, 15, 16]. Our work has focused on digital histological slides of breast cancer as a case study for developing machine vision systems. In particular, slides stained with H-E and Ki-67 serve as the basis for evaluating algorithm performance and ensuring diagnostic precision [17]. Additionally, machine learning has found broad application in digital pathology [18, 19].

The Ki-67 marker is widely recognized as both a predictive and prognostic biomarker in breast carcinoma. It is commonly used to assess cellular proliferation [20, 21], with elevated levels indicating a poorer prognosis [22]. Endorsed by the 2009 St. Gallen International Breast Cancer Conference [23], the use of proliferation markers like Ki-67 informs optimal treatment decisions for early-stage breast cancer. The Ki-67 index is calculated as the ratio of Ki-67-positive tumor cells to the total tumor cell count, or:

$$\text{Ki67} = \frac{\text{Number of cells positive to Ki-67}}{\text{Total number of tumor cells}} \cdot 100, \tag{1}$$

and it is typically estimated in clinical practice either by an *average* method, where pathologists count positive cells across several regions of a slide, or by the *hotspot* method, which focuses on areas with particularly intense staining [24]. Recent studies [25] suggest that a Ki-67 level above 10-14% indicates

[1] https://5000genomivda.it/en/

a high-risk prognosis, but these thresholds remain a subject of ongoing debate[26], complicating the standardization of manual and automated scoring systems. The International Ki-67 Working Group (IKWG) proposes Ki-67 cutoffs of 5% and 30% for prognosis, with intermediate values considered a "gray zone" [27]. At U. Parini Hospital (Aosta), a 20% threshold is commonly used; around this level, therapeutic decisions require comprehensive clinical evaluation beyond the Ki-67 index. High inter-observer variability in classification and differences in threshold selection further hinder reliable assessment [28]. Threshold variability for risk stratification and inter-laboratory differences—such as region-of-interest selection—complicate evaluation of automated tools.

Several computational solutions support automated Ki-67 quantification. Among open-source options, `QuPath` [29] - which uses the `StarDist` algorithm for cell detection - has been widely employed in studies comparing manual scoring and digital image analysis [30, 31, 32, 33]. Our work integrates this detection model into a custom system tailored for the hospital's clinical workflow, encompassing data management, high-performance computing (HPC) processing, and modules for cell normalization and filtering. Other deep learning approaches (e.g. YOLO[34], VGG networks[35], and U-Net with ResNet backbones[36]) focus on nucleus-level classification rather than reporting a whole-slide Ki-67 index. Finally, commercial closed-source platforms (e.g. Visiopharm and DeepBio) designed for clinical use employ proprietary algorithms, but their methods and validation data are often undisclosed.

2.2. CAD in clinical practice

Computer-Aided Diagnosis (CAD) is an advanced field in medical imaging that uses digital imaging and artificial intelligence algorithms to support healthcare professionals in interpreting complex medical images [37, 38, 39]. CAD systems have been widely adopted for the quantitative assessment of immunohistochemical staining, facilitating the identification and measurement of biomarkers critical for diagnosis [12]. Recent developments have expanded these systems to include the analysis of standard hematoxylin and eosin (H-E) images, which form the foundation of pathological diagnosis [40, 41]. By integrating advanced algorithms, CAD improves diagnostic accuracy and decision making, enabling the detection of subtle patterns and anomalies that may be difficult to discern with the naked eye [42, 15]. Furthermore, this approach improves efficiency by streamlining image analysis and allowing clinicians to devote more time to complex diagnostic tasks.

In the context of local clinical practice, particularly in resource-limited or remote settings, such as in mountain regions, CAD offers significant benefits by providing reliable and automated support that complements the expertise of local clinicians. Our system, while innovative, has been designed with the specific intention of integrating seamlessly into existing clinical workflows without causing disruption. For this work, our multidisciplinary team has worked closely with clinical partners, notably the Specialized Unit of Pathological Anatomy[2] in Aosta, to translate clinical requirements into effective CAD tools. This collaboration has ensured that our machine vision algorithms are not only effective in real-world contexts but also respect and accommodate common clinical practices, reinforcing rather than interfering with the essential role of clinical judgment in patient care [43, 44, 45].

2.3. European and regional relevance

Mountain regions face significant challenges, notably limited access to specialist care, which necessitates the adoption of innovative technologies such as AI-driven machine vision and CAD tools. European best practices and regulatory frameworks support this integration by promoting multi-stakeholder collaboration and user-centered design. An European Parliament study [46] proposes engaging clinicians, patients, social scientists, and regulators throughout the development process while also emphasizing enhanced education programs to improve AI literacy among healthcare professionals and the public. Similarly, the new European AI Act calls for the development of harmonized guidelines and standards through close collaboration between AI developers, healthcare professionals, and patient communities to ensure effective monitoring of health-related AI applications [47]. Complementing these initiatives,

[2] "Struttura complessa di Anatomia Patologica" is the formal name of the unit at the hospital.

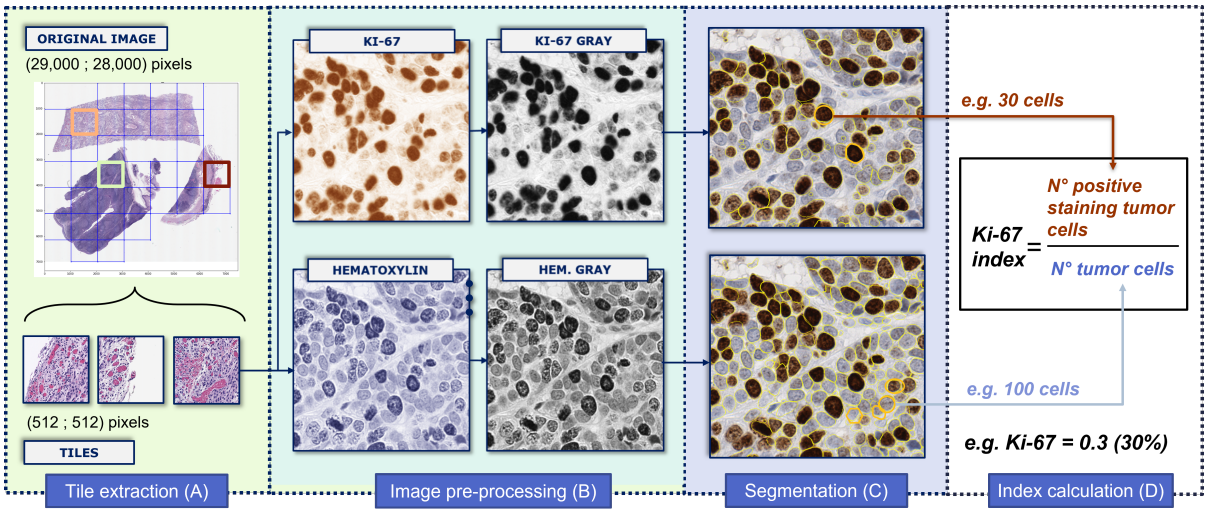

Figure 1: General workflow of the developed process: from left to right, the normalized extracted tile (A), followed by the dye separation phase (B) and subsequent grayscale conversion, which serve as inputs for the tile segmentation phase (C), and finally, cell counting (D). Image from the `DataVal` dataset.

the Standing Committee of European Doctors (CPME) guidelines[3] stress that AI systems must be designed based on actual healthcare demands, and to adhere to ethical and data protection standards. Finally, the white paper Sustainable AI to Drive Global Health[4] underscores the transformative potential of data and AI in addressing global health challenges.

Collectively, these frameworks provide a comprehensive road-map for deploying AI in under-served mountain regions, ensuring that technological advancements are tailored to overcome local health-care disparities while aligning with international best practices. Emerging evidence indicates that the integration of AI-driven machine vision and CAD systems can substantially improve healthcare outcomes in logistically-complex mountain regions. For example, studies have shown that telemedicine and AI-assisted diagnostics can enhance diagnostic accuracy and facilitate timely treatment [48, 49]. Emerging evidence indicates that practical implementation of AI in medicine leads to earlier disease detection and improved patient outcomes, ultimately enhancing quality of life [50]. Moreover, AI integration streamlines data sharing and promotes interdisciplinary collaboration, strengthening ties between hospitals and research institutions [51]. Collectively, these advances not only optimize resource allocation and reduce costs but also contribute to broader economic and social development in mountain regions.

3. Machine Vision for Computer-Aided Diagnosis

In this Section, we describe the workflow developed for the machine vision tool to segment nuclei and compute the Ki-67 index. For a detailed overview of the workflow, please see Figure 1.

3.1. Data

A representative dataset of histological samples stained with hematoxylin and Ki-67 was used during the development phase. This dataset [52], called `DataDev` consists of $N_{\text{DataDev}} = 694$ images, each measuring 512×512 pixels, obtained from samples of 32 patients with breast cancer. This dataset was used to calibrate the system's parameters based on a semi-qualitative assessment of the segmentation, combining statistical analysis with visual inspection. For the results and the clinical validation phase, a different dataset, `DataVal`, was provided by the U. Parini hospital, with each slide accompanied

[3] https://www.cpme.eu/api/documents/adopted/2024/11/cpme_ad_09112024_073.final.policy.on.deployment.of.ai.in.healthcare.pdf

[4] https://www.feam.eu/wp-content/uploads/Sustainable-AI-to-Drive-Global-Health-white-paper-11-Sep.pdf

by a Ki-67 index assigned by expert pathologists. This dataset comprises $N_{\text{DataVal}} = 13$ anonymised histological slides from tumor biopsies performed on female patients diagnosed with breast cancer[5]. Both dataset represent breast cancer cases at different stages of aggressiveness. The machine vision system was customised and optimised on the `DataDev` dataset and subsequently validated in a blinded manner on the `DataVal` dataset provided by the hospital; the validation dataset was used exclusively for evaluation, without any involvement in the calibration phase.

Data preparation and annotation for `DataVal` dataset. Hematoxylin-Ki-67 stained slides were prepared by incubating them with a chromogenic substrate, such as DAB, until the desired color developed (typically 5–10 minutes), with the brown DAB chromogen highlighting proliferating cells. A light hematoxylin counterstain was then applied to enhance the histological context, binding to all nuclei to facilitate histological analysis. The slides from the research dataset and the test image were digitized using the Aperio AT2 scanner[6]. The process involved setting the scanner parameters, including a magnification of 20X or 40X and saving images as `.svs` format. The digitized images were then assigned a clinical Ki-67 index, determined by medical professionals through microscopic observation. The combined workflow of histological preparation, staining, digitization, and clinical annotation ensures the quality and accuracy of subsequent analyses for both diagnosis and research. A distinctive feature of these images is their pyramidal structure, where each image contains multiple resolution levels, allowing access to different versions with varying detail. The choice of resolution level also depends on the magnification used during digitization (20X or 40X) and the specific size of the acquired slide. For this study, analysis was conducted at level 0 (maximum resolution) to ensure the highest level of detail for histological sample evaluation. As reference, a magnification of 40X (20X) corresponds to a resolution of $0.25\mu m$/pixel ($0.5\mu m$/pixel).

3.2. Architecture and algorithm details

The machine vision system is designed as a modular pipeline for processing digitized histological slides to compute proliferation indices. The libraries used in the pipeline include `OpenSlide`[7] for opening and managing image files, `Scikit-image`[8] for creating masks to remove non-biological tissue areas, `DeepZoom`[9] for tile extraction, `SciPy`[10] and `Scikit-learn`[11] for stain separation and other image processing tasks such as color deconvolution and normalization, finally `StarDist` for image segmentation. A workflow of the machine vision pipeline is reproduced in Figure 1.

A. Tile extraction. The images produced by the Aperio scanner are ultra-high-resolution, often too large to be processed in a single operation. To make processing more manageable, tiling is used to divide the original image into smaller, more manageable sections, called "tiles." Each tile retains the original resolution, allowing for detailed analysis without losing important information. During tile extraction, non-biological regions are removed, focusing only on relevant tissue regions. This step is crucial as it significantly reduces computational load, enabling subsequent algorithms to operate more efficiently. To prevent nuclei from being cut at tile boundaries and causing segmentation errors, an overlap method was implemented. However, final results indicate that this effect does not significantly impact the final Ki-67 computation.

[5] All 13 patients provided written informed consent - *consenso informato* - allowing the use of their sensitive data for research purposes. In compliance with ethical guidelines, all images were anonymised, ensuring that only the hospital's medical staff had access to patients' identities and sensitive information.

[6] https://www.leicabiosystems.com/sites/default/files/2020-10/Aperio_AT2_Brochure_USA.pdf

[7] https://openslide.org/api/python/

[8] https://scikit-image.org/docs/stable/api/skimage.html

[9] https://github.com/openzoom/deepzoom.py

[10] https://scipy.org/

[11] https://scikit-learn.org/stable/index.html

B. Image pre-processing: stain separation and normalization. Histological images can vary significantly in coloration due to differences in staining protocols, acquisition conditions, or scanner types. Tile normalization standardizes image coloration, ensuring comparability across samples and preventing color variations from affecting automated analysis [53]. This process relies on a reference image representing the desired chromatic standard, adjusting each tile to match it as closely as possible by correcting brightness, contrast, and hue. For this work, we used the normalization method as in [54]. The result is a dataset with uniform chromatic properties, improving the reliability of subsequent analyses. Histological images are typically stained with specific dyes to highlight different cellular components. Hematoxylin stains cell nuclei in blue or purple, while eosin colors the cytoplasm, connective tissue, and other structures in shades of pink. Ki-67 selectively stains proliferating cell nuclei in brown, making them identifiable within the histological sample (see some examples in Figure 2). Stain separation, or color deconvolution, isolates the chromatic information associated with each dye. This technique is particularly useful for converting images into grayscale representations, where each channel corresponds to a single stain.

C. Nuclei segmentation and feature extraction. After stain separation, each tile produced two grayscale images: one highlighting Ki-67 staining, and the other emphasizing hematoxylin. Segmentation is then performed to automatically identify cell nuclei, a crucial step for calculating the Ki-67 index [55, 56]. The segmentation algorithms detect the darkest areas in the grayscale images, corresponding to cell nuclei—either those stained with hematoxylin, appearing purple, or those marked by Ki-67, appearing brown.

The segmentation process was performed using `StarDist`, a deep learning-based algorithm designed for the detection of star-convex objects, particularly useful for segmenting cell nuclei in histological images. `StarDist` utilizes a convolutional neural network (CNN) to predict the shape and location of nuclei, allowing for precise delineation of overlapping or irregularly shaped nuclei through star-convex polygons. This method has shown superior performance over traditional segmentation techniques in various biological image analysis tasks [57]. The code was customized to suit our processing pipeline and evaluated on `DataDev` dataset - taken advantages of the pre-trained neural network weights already present in the code distribution. Validation was then conducted on the `DataVal` dataset, by comparing the automated results to manual annotations demonstrating the algorithm's accuracy and reliability for segmenting cell nuclei in this study (see Sec. 4). The implementation used in this work is based on the open-source version of the code[12].

The segmentation algorithm creates a table containing various morphological properties of the detected nuclei, including area, perimeter, ellipticity, and color intensity. This data is used for filtering, selecting only nuclei with specific characteristics. Filtering is essential to focus on relevant cells, as without it, segmentation would produce an inaccurate count, mistakenly identifying all cells in the slide instead of only those of interest. To ensure the algorithm correctly distinguishes and counts only the relevant cells, thresholds were applied based on three properties: area, staining intensity, and ellipticity.

D. Proliferation index calculation. To calculate the Ki-67 index, the property tables generated by the segmentation algorithm were used to automatically count the cells in the segmented images. Specifically, the numerator of the formula (see Eq (1)) was obtained by counting the segmented elements from the grayscale image derived from the Ki-67 stain separation. Similarly, the denominator was calculated by counting the segmented elements from the grayscale image derived from the hematoxylin stain separation. For some example of nuclei segmentation and index computation see Figure 2.

This system was tested on the High-Performance Computing (HPC) cluster at Pont-Saint-Martin, utilizing GPU nodes for optimized processing. Execution times for pre-processing and segmentation were recorded, with an average of 8 minutes for pre-processing and 16 minutes for segmentation and Ki-67 extraction, both deemed suitable for clinical workflows.

[12] https://github.com/stardist/stardist

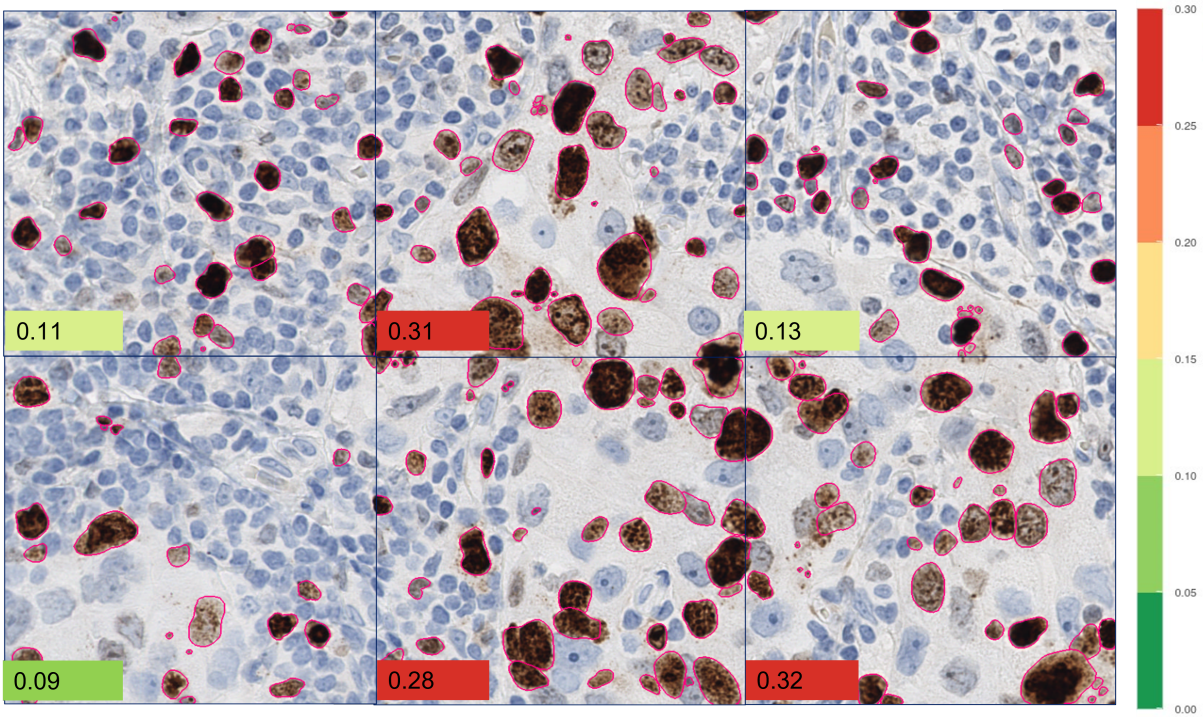

Figure 2: Examples of tiles from the research dataset segmented by the algorithm. The pink circle highlights the identified nuclei. The colored number in the lower left of each tile represents the automatically calculated Ki-67 index based on nuclei count. The number's color reflects the level of the Ki-67 index according to the color scale shown on the right. Images are from the `DataDev` dataset.

3.3. CAD implementation

The CAD system is implemented as a web-based application accessible via a secure VPN, restricted to authorized personnel authenticated through access credentials. It ensures proper data handling in compliance with current regulations, including GDPR[13]. The system is deployed on an HPC cluster and structured using `Singularity/Apptainer` containers. Web apps were developed using `Dash-Plotly`[14], a `Python` library and framework for publishing and visualizing data through a website. The backend of `Dash` is built on `Flask`[15], a lightweight web application framework, while the frontend consists of a static web page populated with `React` components, which provide interactivity to users without the need for a full-page reload[16].

The application features two dashboards: one for image upload and high-resolution preview, and another interactive viewer displaying processed results, including nuclear segmentation metrics and Ki-67 values. Upon image upload, metadata is stored in a backend database, and the file is saved on the HPC. Processing is automated, generating segmentation and proliferation data. The interactive viewer enables clinicians to select regions of interest (ROIs) and obtain real-time Ki-67 index updates, facilitating focused analysis. Designed to integrate seamlessly into existing clinical workflows, the interface provides clear visualizations and actionable data to support clinical decision-making.

[13] https://www.edps.europa.eu/data-protection/our-work/subjects/health_en
[14] https://dash.plotly.com/
[15] https://flask.palletsprojects.com/en/stable/
[16] In more details, `Dash-Plotly` handles the frontend and data exchange between the frontend and backend. The lifecycle of each application is managed by `uWSGI`, an application server that provides load balancing and health check functionalities. To complete the stack, `Nginx` was chosen as the web server for its native support of the WSGI protocol. Nginx also provides data compression, offloading both the network and the `Python` application.

4. Results and validation

The algorithm aims to compute the Ki-67 index for entire whole-slide images. `DataDev` contains nuclei annotated for Ki-67 positivity, extracted as cropped regions from externally sourced slides with varying sizes and quality. To prevent overfitting, we did not retrain the StarDist model on `DataDev`. Instead, we used `DataDev` to calibrate nucleus detection by tuning post-segmentation filters on mean intensity (> 80 on a 0–255 scale), area (150–4000 pixels), and ellipticity (> 0.2). These thresholds were chosen based on descriptive statistics, qualitative inspection of segmentation results, and expert pathologist feedback.

The system's performance was evaluated using the `DataVal` dataset. Nuclear segmentation outputs were assessed both quantitatively and qualitatively by comparing segmented nuclei and their statistical properties per tile. Visual inspection by expert pathologists at the hospital confirmed accurate identification of most nuclei, although some misclassifications occurred with non-tumoral structures (e.g., red blood cells, lymphocytes). Introducing morphological thresholds significantly improved segmentation accuracy by excluding these artifacts. Importantly, the `DataVal` dataset was used exclusively for evaluation, without any involvement in training or optimization of the machine vision system.

The Ki-67 index computation was validated by comparing system-generated values with those assigned by pathologists, Figure 3. Due to the limited sample size ($n = 13$), we compared automated and annotated Ki-67 indices using a ±5% discrepancy threshold, selected in consultation with expert pathologists. This threshold reflects a clinically meaningful margin and aligns with inter-laboratory variability and IKWG guidelines [27, 28]. While the automated calculation closely aligned with expert assessments in most cases, two out of 13 images exhibited discrepancies exceeding 5%: patients 4 (id: I2304166) and 5 (id: I2302878). In patient 4, clinical values remain high (around 70%), while the algorithm tends to underestimate Ki-67. For patient 5, the clinical value is approximately 10%, whereas algorithm estimates are 28% at 40X magnification and 37% at 20X. This prompted an exploration of alternative region selection methods, such as hotspot and bootstrap-based approaches, to refine Ki-67 computation. Error analysis revealed that a major source of error was the inclusion of regions that are not clinically relevant or contain tumor cells which should not be counted for Ki-67. This is consistent with the performance variability depending on whether regions of interest are preselected, as demonstrated in reported studies using tools like `QuPath` (see Sec. 2.1). To address this, we kept the automated cell segmentation and counting system active for index computation while integrating a CAD tool for selecting relevant areas. This web application enables clinicians to upload images, define regions of interest, and receive index computations within minutes.

4.1. Clinical validation and impact

The validation of the system demonstrates its significant clinical utility by ensuring accurate, reproducible, and efficient quantification of the Ki-67 index, a key biomarker in breast cancer diagnosis and prognosis. Through a comprehensive validation process that compared automated Ki-67 calculations with expert pathologist annotations, the system proved its reliability in assisting routine pathological assessments. The system was ultimately deployed to hospital via a dedicated web application. This web app, developed as a CAD tool, enables (only) authenticated clinicians at Parini hospital to access the system remotely via VPN, providing an interactive platform for uploading, processing, and visualizing histopathological images. The application allows real-time visualization of whole-slide images, displays segmentation results, and provides a detailed breakdown of the Ki-67 index for each analyzed region (for an example, see Figure 4).

By automating and standardizing Ki-67 quantification, the tool significantly reduces inter-observer variability and minimizes diagnostic subjectivity, enhancing diagnostic confidence, particularly in borderline cases. Moreover, it improves workflow efficiency, allowing pathologists to focus on more complex evaluations rather than time-consuming manual quantifications. The validation process also identified and addressed challenges such as misclassification of non-tumoral cells and discrepancies in region selection. To enhance accuracy, the system incorporates morphological thresholds to refine segmentation and enables manual selection of regions of interest (ROI) for Ki-67 calculation, ensuring

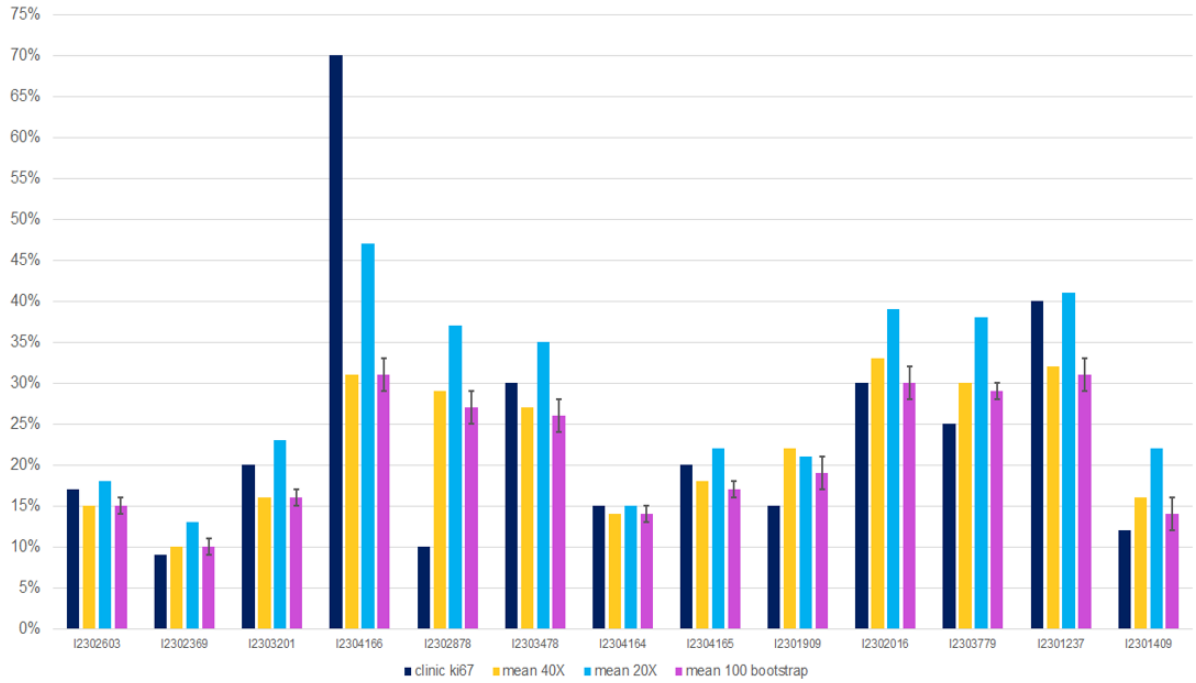

Figure 3: The bar graph presents, for each image, the Ki-67 value assigned by an expert pathologist (dark blue) alongside the value computed as the mean of Ki-67 estimates obtained from each tile within the automatically selected ROIs using a bootstrap method (40X resolution, magenta) to assess variance of the index Ki-67 automatic computation. Additionally, the mean values calculated over the entire slide at 20X (light blue) and 40X (yellow) resolutions are reported.

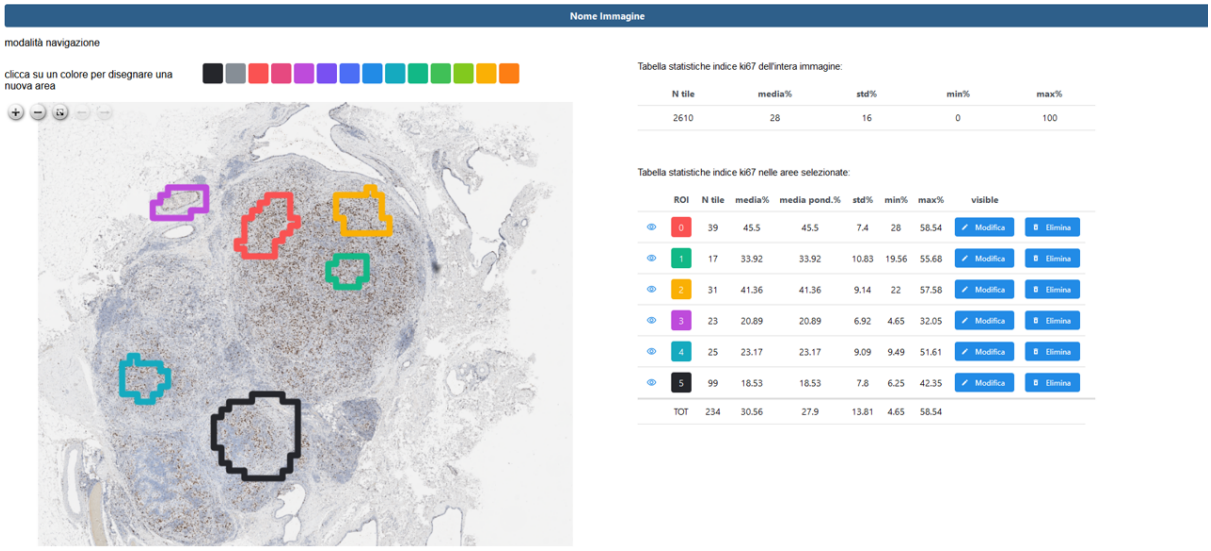

Figure 4: Web app interface of the CAD tool for visualizing histological images and calculating the Ki-67 index.

alignment with clinical best practices. Additionally, the web app's structured data storage and retrieval system facilitates longitudinal analysis and integration with hospital databases, potentially supporting further predictive analytics and research applications.

The deployment of this web-based CAD tool represents a step toward integrating AI-driven solutions into clinical practice, enabling real-time, evidence-based decision-making. While the system demonstrated robust performance, ongoing evaluations in clinical settings will further refine its capabilities and address limitations. Future improvements may include AI-assisted ROI selection and deep-learning enhancements for more precise segmentation.

5. Discussion: scientific, socio-economic, and community Impact

5.1. Scientific contributions and interdisciplinary collaboration

Our study demonstrates significant advances in AI-driven medical [18, 19] imaging by developing an innovative CAD system practically implemented within the clinical workflow, that automates high-resolution histological analysis and precise quantification of the Ki-67 proliferation index [38, 12]. A first validation against expert pathologist annotations confirmed its clinical utility, notably reducing inter-observer variability and diagnostic subjectivity [42, 15]. Comprehensive validation of the system impact will be a key focus of future work, which aims to systematically assess detection performances as well as clinical utility and user experience. The system is designed to efficiently collect statistical results and expert-selected regions, enabling future model retraining and optimization for the specific use case, as well as more meaningful performance evaluations. Moreover, the deployment of a secure, web-based CAD tool facilitates real-time access and analysis, further bridging the gap between technological innovation and clinical practice. This work contributes to the expanding research on CAD systems and exemplifies the power of interdisciplinary collaboration in addressing complex clinical challenges, particularly in resource-limited settings [47].

5.2. Economic and social benefits

This pilot study underscores the potential for technology transfer and innovative research to drive local economic growth in mountain regions. By focusing on the computation of the Ki-67 proliferation index, our CAD platform not only enhances diagnostic accuracy but also lays the foundation for a comprehensive digital pathology infrastructure - one that can facilitate secure image sharing among clinicians and spur the development of new digital health services. In line with European regulations and ethical guidelines governing AI in clinical settings [46], our system was developed following best practices that ensure both scientific integrity and clinical reliability. Furthermore, the implementation of such cutting-edge technology can foster job creation and stimulate local markets while significantly improving the quality of care, community resilience, and sustainable development in mountain territories like the Aosta Valley.

5.3. Clinical and regional impact

The CAD tool significantly enhances diagnostic accuracy and supports local clinicians in under-resourced mountain regions by fostering a collaborative environment where machine-based analysis and expert human judgment work synergistically [43]. Its streamlined platform enables easy sharing of digital images, facilitating second opinions and external consultation, which is particularly valuable in small, low-population areas where clinicians may encounter fewer complex cases. This system not only improves workflow efficiency but also ensures that even rare or challenging diagnostic scenarios receive expert review, ultimately boosting the quality of care and promoting regional resilience [50].

5.4. Future prospects

Future developments of the CAD system will focus on scalability and expanding its diagnostic capabilities on other case studies rather than breast cancer, e.g. lung or prostate cancer. One promising direction is the integration of additional biomarkers, such as the evaluation of PD-L1 expression in tumor cells, which plays a critical role in immunotherapy decision-making. Incorporating other imaging modalities and advanced deep-learning techniques could further enhance the system's clinical utility, transforming it into a comprehensive digital pathology platform. Strengthening collaborations between local institutions, research organizations, and industry partners will be essential to driving innovation, fostering technological advancements, and promoting sustainable healthcare solutions. These efforts will not only improve diagnostic accuracy and efficiency but also contribute to the long-term development of digital health services in remote and underserved regions.

In parallel, a more comprehensive evaluation is planned. This will involve a systematic assessment of the system's performance in comparison with other software solutions and expert annotations. The ongoing collection of data and results through the CAD tool usage will enable this evaluation and also support future model refinement, contributing to the advancement of automated Ki-67 quantification also from a scientific perspective.

6. Conclusion

This study presented a machine vision CAD tool designed to compute the Ki-67 index from digitized histopathological images. Developed as a web-based platform, the system facilitates seamless integration into clinical workflows, enabling automated and standardized quantification. Validation against hospital-provided images demonstrated strong concordance with expert assessments, confirming its reliability as a diagnostic support tool. Beyond its clinical impact, the platform fosters interdisciplinary collaboration and exemplifies how AI-driven innovations can enhance healthcare accessibility in mountainous regions. By promoting digital pathology, second-opinion consultations, and efficient diagnostics, this initiative supports both scientific progress and regional healthcare development. Continued research and collaboration will be key to expanding the system's capabilities and results validation, ensuring its long-term impact in both local and broader medical and scientific contexts.

Acknowledgments

The OAVdA[17] is managed by the Fondazione Clément Fillietroz-ONLUS, which is supported by the Regional Government of the Aosta Valley, the Town Municipality of Nus and the "Unité des Communes valdôtaines Mont-Émilius". We acknowledge that all simulations, machine vision development, and testing were performed on the CMP3@vda - 5000genomi project High Performance Computing (HPC) cluster, managed by Engineering D.HUB. 5000genomi@VdA is a scientific project that has enabled the creation of a new research Center dedicated to Personalized, Preventive and Predictive Medicine (CMP3VdA) for neurodevelopmental, neurodegenerative and oncological diseases. 5000genomi@VdA is carried out by a research consortium led by IIT-Istituto Italiano di Tecnologia (Italian Institute of Technology), comprising Universitá della Valle d'Aosta, Cittá della Salute e della Scienza di Torino, Fondazione Clément Fillietroz-ONLUS, and Engineering D.HUB.

Declaration on Generative AI

This document was reviewed using generative AI strictly for grammar and text revision, ensuring clarity and coherence without altering the original content or analysis.

References

[1] American Cancer Society, Breast Cancer Early Detection and Diagnosis, 2023. Retrieved from https://www.cancer.org.

[2] N. F. Boyd, H. Guo, L. J. Martin, et al., Mammographic density and the risk and detection of breast cancer, New England Journal of Medicine 356 (2007) 227–236. doi:10.1056/NEJMoa062790.

[3] S. Ciatto, N. Houssami, D. Bernardi, et al., Integration of 3d digital mammography with tomosynthesis for population breast-cancer screening (storm): A prospective comparison study, The Lancet Oncology 14 (2013) 583–589. doi:10.1016/S1470-2045(13)70134-7.

[4] V. Suciu, C. El Chamieh, R. Soufan, M.-C. Mathieu, C. Balleyguier, S. Delaloge, Z. Balogh, J.-Y. Scoazec, S. Chevret, P. Vielh, Real-world diagnostic accuracy of the on-site cytopathology advance

[17] https://www.oavda.it/

report (oscar) procedure performed in a multidisciplinary one-stop breast clinic, Cancers 15 (2023) 4967. URL: http://dx.doi.org/10.3390/cancers15204967. doi:10.3390/cancers15204967.

[5] S. J. Schnitt, T. W. Jacobs, Pathology of breast cancer: a review, The American Journal of Surgical Pathology 43 (2019) 757–766.

[6] C. W. Elston, I. O. Ellis, Pathological features of breast cancer, European Journal of Cancer 27 (1991) 123–130.

[7] P. A. Carney, D. L. Miglioretti, B. C. Yankaskas, et al., Individual and combined effects of age, breast density, and hormone replacement therapy use on the accuracy of screening mammography, Annals of Internal Medicine 138 (2003) 168–175. doi:10.7326/0003-4819-138-3-200302040-00008.

[8] S. R. Cummings, et al., The future of cancer screening: biomarkers and early detection, Cancer Epidemiology, Biomarkers and Prevention 26 (2017) 1–10. doi:10.1158/1055-9965.EPI-16-0603.

[9] N. L. Henry, D. F. Hayes, Cancer biomarkers, Molecular Oncology 6 (2012) 140–146. doi:10.1016/j.molonc.2012.01.010.

[10] J. K. C. Chan, The wonderful colors of the hematoxylin-eosin stain in diagnostic surgical pathology, Int. J. Surg. Pathol. 22 (2014) 12–32.

[11] C. R. Taylor, S.-R. Shi, B. Chaiwun, L. Young, S. Imam, R. J. Cote, Strategies for improving the immunohistochemical staining of various intranuclear prognostic markers in formalin-paraffin sections: Androgen receptor, estrogen receptor, progesterone receptor, p53 protein, proliferating cell nuclear antigen, and ki-67 antigen revealed by antigen retrieval techniques, Human Pathology 25 (1994) 263–270. URL: http://dx.doi.org/10.1016/0046-8177(94)90198-8. doi:10.1016/0046-8177(94)90198-8.

[12] A. C. Dufour, A. H. Jonker, J.-C. Olivo-Marin, Deciphering tissue morphodynamics using bioimage informatics, Philosophical Transactions of the Royal Society B: Biological Sciences 372 (2017) 20150512. URL: http://dx.doi.org/10.1098/rstb.2015.0512. doi:10.1098/rstb.2015.0512.

[13] E. Meijering, A. E. Carpenter, H. Peng, F. A. Hamprecht, J.-C. Olivo-Marin, Imagining the future of bioimage analysis, Nature Biotechnology 34 (2016) 1250–1255. URL: http://dx.doi.org/10.1038/nbt.3722. doi:10.1038/nbt.3722.

[14] A. Kan, Machine learning applications in cell image analysis, Immunology & Cell Biology 95 (2017) 525–530. URL: http://dx.doi.org/10.1038/icb.2017.16. doi:10.1038/icb.2017.16.

[15] G. Litjens, T. Kooi, B. E. Bejnordi, A. A. A. Setio, F. Ciompi, M. Ghafoorian, J. A. van der Laak, B. van Ginneken, C. I. Sánchez, A survey on deep learning in medical image analysis, Medical Image Analysis 42 (2017) 60–88. URL: http://dx.doi.org/10.1016/j.media.2017.07.005. doi:10.1016/j.media.2017.07.005.

[16] S. A. Alowais, S. S. Alghamdi, N. Alsuhebany, T. Alqahtani, A. I. Alshaya, S. N. Almohareb, A. Aldairem, M. Alrashed, K. Bin Saleh, H. A. Badreldin, M. S. Al Yami, S. Al Harbi, A. M. Albekairy, Revolutionizing healthcare: the role of artificial intelligence in clinical practice, BMC Med. Educ. 23 (2023) 689.

[17] S. S. Alahmari, D. Goldgof, L. O. Hall, P. R. Mouton, A review of nuclei detection and segmentation on microscopy images using deep learning with applications to unbiased stereology counting, IEEE Transactions on Neural Networks and Learning Systems 35 (2024) 7458–7477. URL: http://dx.doi.org/10.1109/TNNLS.2022.3213407. doi:10.1109/tnnls.2022.3213407.

[18] A. Esteva, et al., Dermatologist-level classification of skin cancer with deep neural networks, Nature 542 (2017) 115–118.

[19] B. E. Bejnordi, et al., Diagnostic assessment of deep learning algorithms for detection of lymph node metastases in women with breast cancer, JAMA 318 (2017) 2199–2210.

[20] M. C. U. Cheang, S. K. Chia, D. e. a. Voduc, Ki67 index is a strong predictor of breast cancer survival in the ncic ctg ma.21 trial, Breast Cancer Research 11 (2009) R87. doi:10.1186/bcr2425.

[21] S. E. Pinder, et al., The prognostic value of ki67 in breast cancer: a meta-analysis, Breast Cancer Research and Treatment 81 (2003) 253–266.

[22] M. Dowsett, et al., Prognostic value of ki67 in breast cancer: a systematic review of the literature, Breast Cancer Research 13 (2011) R105.

[23] A. Goldhirsch, J. Ingle, R. Gelber, A. Coates, B. Thürlimann, H.-J. Senn, Thresholds for therapies:

highlights of the st gallen international expert consensus on the primary therapy of early breast cancer 2009, Annals of Oncology 20 (2009) 1319–1329. URL: http://dx.doi.org/10.1093/annonc/mdp322. doi:10.1093/annonc/mdp322.

[24] B. e. a. Nitzsche, Comparative analysis of ki67 assessment by automated and manual methods in breast cancer, Breast Cancer Research and Treatment 165 (2017) 99–108. doi:10.1007/s10549-017-4238-4.

[25] T. O. Nielsen, S. C. Y. Leung, D. L. Rimm, A. Dodson, B. Acs, S. Badve, C. Denkert, M. J. Ellis, S. Fineberg, M. Flowers, H. H. Kreipe, A.-V. Laenkholm, H. Pan, F. M. Penault-Llorca, M.-Y. Polley, R. Salgado, I. E. Smith, T. Sugie, J. M. S. Bartlett, L. M. McShane, M. Dowsett, D. F. Hayes, Assessment of ki67 in breast cancer: Updated recommendations from the international ki67 in breast cancer working group, J. Natl. Cancer Inst. 113 (2021) 808–819.

[26] E. Rewcastle, I. Skaland, E. Gudlaugsson, S. K. Fykse, J. P. Baak, E. A. Janssen, The ki67 dilemma: investigating prognostic cut-offs and reproducibility for automated ki67 scoring in breast cancer, Breast Cancer Research and Treatment 207 (2024) 1–12.

[27] T. O. Nielsen, S. C. Y. Leung, D. L. Rimm, A. Dodson, B. Acs, S. Badve, C. Denkert, M. J. Ellis, S. Fineberg, M. Flowers, et al., Assessment of ki67 in breast cancer: updated recommendations from the international ki67 in breast cancer working group, JNCI: Journal of the National Cancer Institute 113 (2021) 808–819.

[28] C. M. Focke, H. Bürger, P. J. van Diest, K. Finsterbusch, D. Gläser, E. Korsching, T. Decker, M. Anders, R. Bollmann, F. Eiting, et al., Interlaboratory variability of ki67 staining in breast cancer, European Journal of Cancer 84 (2017) 219–227.

[29] P. Bankhead, M. B. Loughrey, J. A. Fernández, Y. Dombrowski, D. G. McArt, P. D. Dunne, S. McQuaid, R. T. Gray, L. J. Murray, H. G. Coleman, et al., Qupath: Open source software for digital pathology image analysis, Scientific reports 7 (2017) 1–7.

[30] C. Boyaci, W. Sun, S. Robertson, B. Acs, J. Hartman, Independent clinical validation of the automated ki67 scoring guideline from the international ki67 in breast cancer working group, Biomolecules 11 (2021) 1612.

[31] B. Acs, V. Pelekanou, Y. Bai, S. Martinez-Morilla, M. Toki, S. C. Leung, T. O. Nielsen, D. L. Rimm, Ki67 reproducibility using digital image analysis: an inter-platform and inter-operator study, Laboratory Investigation 99 (2019) 107–117.

[32] A. H. Skjervold, H. S. Pettersen, M. Valla, S. Opdahl, A. M. Bofin, Visual and digital assessment of ki-67 in breast cancer tissue-a comparison of methods, Diagnostic Pathology 17 (2022) 45.

[33] T. Koopman, H. J. Buikema, H. Hollema, G. H. de Bock, B. van der Vegt, Digital image analysis of ki67 proliferation index in breast cancer using virtual dual staining on whole tissue sections: clinical validation and inter-platform agreement, Breast cancer research and treatment 169 (2018) 33–42.

[34] D. M. Muthu, P. Amos, et al., Single shot ai-assisted quantification of ki-67 proliferation index in breast cancer, arXiv preprint arXiv:2503.19606 (2025).

[35] P. L. Narayanan, S. E. A. Raza, A. Dodson, B. Gusterson, M. Dowsett, Y. Yuan, Deepsdcs: Dissecting cancer proliferation heterogeneity in ki67 digital whole slide images, arXiv preprint arXiv:1806.10850 (2018).

[36] K. Benaggoune, Z. A. Masry, J. Ma, C. Devalland, L. H. Mouss, N. Zerhouni, A deep learning pipeline for breast cancer ki-67 proliferation index scoring, arXiv preprint arXiv:2203.07452 (2022).

[37] N. Karssemeijer, G. te Brake, Computer-aided detection in mammography: a review, European Journal of Radiology 57 (2006) 177–186.

[38] K. Doi, Computer-aided diagnosis in medical imaging: Historical review, current status and future potential, Computerized Medical Imaging and Graphics 31 (2007) 198–211. URL: http://dx.doi.org/10.1016/j.compmedimag.2007.02.002. doi:10.1016/j.compmedimag.2007.02.002.

[39] J. Caicedo, S. Cooper, F. Heigwer, S. Warchal, P. Qiu, C. Molnar, A. Vasilevich, J. Barry, H. Bansal, O. Kraus, M. Wawer, L. Paavolainen, M. Herrmann, M. H. Rohban, J. Hung, H. Hennig, J. Concannon, I. Smith, P. Clemons, A. Carpenter, Data-analysis strategies for image-based cell profiling, Nature Methods 14 (2017) 849–863. doi:10.1038/nmeth.4397.

[40] M. Veta, J. P. W. Pluim, P. J. van Diest, M. A. Viergever, Breast cancer histopathology image analysis: A review, IEEE Transactions on Biomedical Engineering 61 (2014) 1400–1411. URL: http://dx.doi.org/10.1109/TBME.2014.2303852. doi:10.1109/tbme.2014.2303852.

[41] P. Khosravi, E. Kazemi, M. Imielinski, O. Elemento, I. Hajirasouliha, Deep convolutional neural networks enable discrimination of heterogeneous digital pathology images, EBioMedicine 27 (2018) 317–328. URL: http://dx.doi.org/10.1016/j.ebiom.2017.12.026. doi:10.1016/j.ebiom.2017.12.026.

[42] A. Janowczyk, A. Madabhushi, Deep learning for digital pathology image analysis: A comprehensive tutorial with selected use cases, Journal of Pathology Informatics 7 (2016) 29. URL: http://dx.doi.org/10.4103/2153-3539.186902. doi:10.4103/2153-3539.186902.

[43] J. Wang, et al., Computer-aided diagnosis of breast cancer: Current status and future directions, Medical Physics 45 (2018) 97–108.

[44] R. M. Nishikawa, Current status and future directions of computer-aided diagnosis in mammography, Computerized Medical Imaging and Graphics 31 (2007) 224–235. URL: http://dx.doi.org/10.1016/j.compmedimag.2007.02.009. doi:10.1016/j.compmedimag.2007.02.009.

[45] R. L. Birdwell, P. Bandodkar, D. M. Ikeda, Computer-aided detection with screening mammography in a university hospital setting, Radiology 236 (2005) 451–457. URL: http://dx.doi.org/10.1148/radiol.2362040864. doi:10.1148/radiol.2362040864.

[46] E. P. D. G. for Parliamentary Research Services., Artificial intelligence in healthcare: applications, risks, and ethical and societal impacts., Publications Office, LU, 2022. URL: https://data.europa.eu/doi/10.2861/568473. doi:10.2861/568473.

[47] H. van Kolfschooten, J. van Oirschot, The eu artificial intelligence act (2024): Implications for healthcare, Health Policy 149 (2024) 105152. URL: http://dx.doi.org/10.1016/j.healthpol.2024.105152. doi:10.1016/j.healthpol.2024.105152.

[48] L. Dumitrache, M. Nae, G. Simion, A.-M. Taloș, Modelling potential geographical access of the population to public hospitals and quality health care in romania, International Journal of Environmental Research and Public Health 17 (2020) 8487. URL: http://dx.doi.org/10.3390/ijerph17228487. doi:10.3390/ijerph17228487.

[49] A. Amjad, P. Kordel, G. Fernandes, A review on innovation in healthcare sector (telehealth) through artificial intelligence, Sustainability 15 (2023) 6655. URL: http://dx.doi.org/10.3390/su15086655. doi:10.3390/su15086655.

[50] J. He, S. L. Baxter, J. Xu, J. Xu, X. Zhou, K. Zhang, The practical implementation of artificial intelligence technologies in medicine, Nature Medicine 25 (2019) 30–36. URL: http://dx.doi.org/10.1038/s41591-018-0307-0. doi:10.1038/s41591-018-0307-0.

[51] K. Shameer, K. W. Johnson, B. S. Glicksberg, J. T. Dudley, P. P. Sengupta, Machine learning in cardiovascular medicine: are we there yet?, Heart 104 (2018) 1156–1164. URL: http://dx.doi.org/10.1136/heartjnl-2017-311198. doi:10.1136/heartjnl-2017-311198.

[52] C. Senaras, M. K. K. Niazi, B. Sahiner, M. P. Pennell, G. Tozbikian, G. Lozanski, M. N. Gurcan, Optimized generation of high-resolution phantom images using cgan: Application to quantification of ki67 breast cancer images, PLOS ONE 13 (2018) e0196846. URL: http://dx.doi.org/10.1371/journal.pone.0196846. doi:10.1371/journal.pone.0196846.

[53] T. A. Azevedo Tosta, P. R. de Faria, L. A. Neves, M. Z. do Nascimento, Computational normalization of h&e-stained histological images: Progress, challenges and future potential, Artificial Intelligence in Medicine 95 (2019) 118–132. URL: https://www.sciencedirect.com/science/article/pii/S093336571830424X. doi:https://doi.org/10.1016/j.artmed.2018.10.004.

[54] M. Salvi, N. Michielli, F. Molinari, Stain color adaptive normalization (scan) algorithm: Separation and standardization of histological stains in digital pathology, Computer Methods and Programs in Biomedicine 193 (2020) 105506. URL: http://dx.doi.org/10.1016/j.cmpb.2020.105506. doi:10.1016/j.cmpb.2020.105506.

[55] Y. Xu, et al., A survey of image segmentation methods, Computer Vision and Image Understanding 122 (2016) 1–26.

[56] D. C. Ciresan, et al., Mitosis detection in breast cancer histology images with deep neural networks,

in: Proceedings of the IEEE International Conference on Computer Vision, 2013, pp. 964–971.
[57] U. Schmidt, M. Weigert, C. Broaddus, G. Myers, Cell detection with star-convex polygons, in: Medical image computing and computer assisted intervention–MICCAI 2018: 21st international conference, Granada, Spain, September 16-20, 2018, proceedings, part II 11, Springer, 2018, pp. 265–273.